Deep–Sea Research I 210 (2024) 104360

Contents lists available at ScienceDirect

Deep-Sea Research Part I

journal homepage: www.elsevier.com/locate/dsri

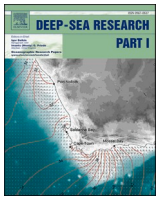

Regional diversity and spatial patterns of epibenthic communities in the Laurentian Channel Marine Protected Area

Sarah N. de Mendonça *, Anna Metaxas

Dalhousie University Department of Oceanography, 1355 Oxford Street, Halifax, NS, B3H 4R2, Canada

A R T I C L E I N F O

Keywords:
Megafauna
Monitoring
Distribution
Assemblage
Ecology
Mapping

A B S T R A C T

Megafauna, such as cold-water corals, can promote diversity through various processes, such as predation, bioturbation, competition, and facilitation as habitat engineers. Further investigation into their ecology and role in epifaunal community structure in the deep sea is needed. Diversity, abundance, and spatial patterns of epibenthic megafauna (≥2 cm) were quantified at regional-scales (100 s m – 100 s km) using high-resolution imagery from 15 stations in the Laurentian Channel Marine Protected Area, Canada. A patchy community structure was significantly associated with station and benthoscape class, which in turn was based on geological factors. Three types of assemblages included: (1) dominated by corals *Pennatula* sp. 2 and/or Hexacorallia (SC.) spp. in shallow eastern benthoscape classes with high abundance and low diversity; (2) a diverse mix of taxa (e.g. sea pens *Anthoptilum* spp. and *Kophobelemnon* spp., anemones/cerianthids, etc.) in deeper (>400 m) western benthoscape classes, with low abundance and high diversity; and (3) a unique community dominated by sponges. Overall, eight taxa contributed to most dissimilarities between stations, and communities were similar within 10 km but could differ at greater distances. Benthoscape classes captured environmental factors (e.g. depth and substrate) that may be responsible for changes in diversity and abundance, and are used as a proxy for different habitats. Our study advanced the understanding of regional spatial patterns in the abundance, composition, and diversity of epibenthic communities, by identifying spatial patterns particularly in the Laurentian Channel where data were limited, adding to interpretations of spatial ecology in a previous fine-scale study. Additionally, these spatial patterns reflect various underlying ecological processes that are mostly unknown. Our community analysis and observed changes in abundance and diversity have implications that can help inform future monitoring designs to promote representative and meaningful spatial assessments.

1. Introduction

Taxonomic diversity is the outcome of a combination of long-term evolutionary (e.g. speciation and geographic dispersal) and short-term ecological processes (e.g. competition and predation) (Levin et al., 2001). In the deep sea, megafauna (invertebrates and fish > 1–2 cm) can promote diversity through multiple processes (predation, bioturbation, competition, and facilitation as habitat engineers) although the relative importance of each process is not well understood (Mcclain and Schlacher, 2015). Several hypotheses have been proposed to explain patterns of diversity in the deep sea, including some that integrate different processes on ecological time scales, such as physical or biological disturbance and niche partitioning through competition or spatial heterogeneity (e.g. Mcclain and Schlacher, 2015; Rex, 1981). The dynamic equilibrium hypothesis integrates productivity, competition, predation, and physical disturbance to explain patterns in diversity (Rex, 1981; Huston, 1979). As depth increases, competitive displacement rates are hypothesized to decrease, with lower diversity on the continental shelf and upper continental slope than the lower slope, as a result of high rates of displacement. In the last few decades, although our knowledge of deep-sea ecosystems and biodiversity has increased substantially, through network initiatives such as iAtlantic (Boteler et al., 2023) and the Census of Marine Life (Snelgrove, 2010) significant gaps still exist, including for cold-water coral communities.

Sea pens are cold-water corals which are primarily sessile and anchor into soft sediments using a peduncle, although several species have been observed retracting into the sea floor. Several species have been estimated to be long lived (2–48 years) with generally slow growth of 1.0 ± 0.09 to 4.9 ± 0.06 cm/year (Greeley, 2022; Murillo et al., 2018; Neves et al., 2015, 2018; Wilson et al., 2002). Sea pens can play an important

* Corresponding author.
E-mail addresses: sarah.de.mendonca@dal.ca (S.N. de Mendonça), metaxas@dal.ca (A. Metaxas).

https://doi.org/10.1016/j.dsr.2024.104360
Received 15 February 2024; Received in revised form 17 June 2024; Accepted 9 July 2024
Available online 10 July 2024

functional role in soft-sediment environments, possibly providing biogenic vertical habitat structure which alters currents, retains nutrients, and provides nurseries and protection for fish (e.g. Baillon et al., 2012; Tissot et al., 2006). In the Northwest Atlantic, sea pen species have been associated with fish (Boulard et al., 2023; Baillon et al., 2012) and macrofauna (Miatta and Snelgrove, 2022).

Several environmental factors have been identified as important drivers in observed distributions and as predictors in regional species distribution models for deep-water corals. These factors include depth, substrate, temperature, salinity, and surface chlorophyll *a* as important predictors of abundance (e.g. Gullage et al., 2017; Lacharité and Metaxas, 2017; Kenchington et al., 2016; Murillo et al., 2016; Greathead et al., 2015; Baker et al., 2012). Other geological variables such as pockmarks, pits in the sediment created by gas or fluid (Fader, 1991), could also play a role in abundance and diversity but have not been thoroughly tested (de Mendonça and Metaxas, 2024; Somoza et al., 2021; Webb et al., 2009; Sumida et al., 2004).

In the deep sea, data on environmental drivers that explain the distribution and diversity of epibenthic megafauna often do not exist in appropriate resolution and proxies are used instead. Benthoscapes can be such a proxy, used to identify patches of seabed, based on biophysical sea floor classification of combinations of biotic (e.g. biogenic structures) and abiotic (e.g. sediment and geomorphic features) components (e.g. Zajac, 2008). Classification is based on a spatial analysis of abiotic and/or biotic data and therefore is a statistical rather than mechanistic tool, where the characteristics of each class are determined through the similarities among specific locations in the region of interest. For example, one benthoscape class may be characterized as deep with abundant ice scours and another as shallow with coarser sediments (Lacharité et al., 2020). Unique epifaunal communities were found in different benthoscape classes in Newfoundland and Labrador, Canada (Proudfoot et al., 2020), fish assemblages on a seamount on the southwest Indian ridge (Swanborn et al., 2023), as well as megafauna in Norway (Mortensen et al., 2009) and the Mauritian continental slope (Jones and Brewer, 2012).

The Laurentian Channel is a cross-shelf trough, located in Atlantic Canada (southwest of Newfoundland) between the St. Lawerence river and the edge of the continental shelf (Todd, 2016). In 2019, the eastern portion of the channel (11 619 km^2) was designated as the Laurentian Channel Marine Protected Area (LC MPA) with one of the conservation priorities being to protect sea pens from human activities (DFO, 2019b). In the eastern half of the Laurentian Channel and the Newfoundland and Labrador shelves, suitable habitats for sea pens, cup corals and soft corals have been projected based on regional distribution models using primarily depth, temperature, salinity, slope, chlorophyll *a*/primary production and trawl biomass data at a coarse resolution as predictors that vary in importance by species (Gullage et al., 2017; Guijarro et al., 2016). Habitat suitability was high for most of the MPA and extended outside the northeastern boundary for both sea pens and cup corals, but was more variable for soft corals. Outside the Laurentian Channel, habitat suitability for sea pens and cup corals was variable along the shelf edge, being overall higher west of the Grand Banks and around the Flemish Cap. Medium to high habitat suitability for soft corals covered a larger part of the continental shelf relative to the LC MPA (Gullage et al., 2017; Guijarro et al., 2016). The Laurentian Channel had the largest areas of significant concentrations of sea pens in the region as identified through trawl (biomass) data (see Fig. 42 in Kenchington et al., 2016), including in more than ¾ of the MPA. Other areas with significant concentrations of sea pens were found in the channel west of the MPA and on the shelf edge southeast of the MPA. Various other invertebrates have also been observed within the channel in past imagery surveys, such as asteroids and anemones (e.g. Lacharité et al., 2020). Also, a benthoscape classification has been developed for the LC MPA which is based on combinations of depth, slope, presence of ice scours and pockmarks, and surficial sediment (Table A2). Relationships between faunal abundance and benthoscape class have not been examined in this region. At present, the Department of Fisheries and Ocean Canada are conducting extensive work towards characterizing the LC MPA and developing a monitoring plan. However, the spatial patterns and ecology in the region are missing, particularly for sea pens.

Estimating the abundance of sea pens is challenging because of their small size, possible retraction behaviour (Kenchington et al., 2011) and flexibility or fragility (Auster et al., 2011). For the Newfoundland region, research trawls have recorded the highest biomass of several sea pen species in the Laurentian Channel, although trawls have low catch efficiency for sea pens (Chimienti et al., 2018; Kenchington et al., 2011). Sea pen biomass was predicted to be up to 24.27 kg in a small portion of the channel but lower elsewhere (Guijarro et al., 2016). High-resolution imagery can provide more accurate measures, as it has a higher capture efficiency than trawls (e.g. sea pens; Chimienti et al., 2018), and can provide insights into distribution and ecology that are not possible with trawl catch weights at a coarse resolution. However, small size and avoidance behaviours can also lead to sampling bias with imagery. Thus, optimal sampling methods vary based on the species of interest, their morphology, and behaviours. Imagery appears to capture abundance and diversity of benthic invertebrates (e.g. sea pens) better than trawls (de Mendonça and Metaxas, 2021; Chimienti et al., 2018), and allow for analyses of spatial patterns through *in situ* observations.

In this study, we investigate the spatial patterns of epibenthic megafaunal assemblages, particularly sea pens, in the Laurentian Channel MPA. Using high resolution imagery we: 1) quantify regional spatial patterns (100 s m - 100s of kms) in community composition, abundance, and diversity; 2) discuss potential drivers of the patterns in diversity and abundance; 3) investigate and interpret how assemblages are related to previously proposed benthoscape classes; and 4) briefly highlight sampling resolution bias. Our study complements previous studies on fine-scale patterns of megafauna (de Mendonça and Metaxas, 2021, 2024), fish and infauna in the LC MPA (Boulard et al., 2023; Miatta and Snelgrove, 2021, 2022). Estimating broad scale spatial variation can be useful for the management of large MPAs. Additional research at multiple scales will also help establish a times series and better understand the ecological drivers and response in epibenthic megafaunal communities.

2. Methods

2.1. Study area

The Laurentian Channel Marine Protected Area (LC MPA) is 11 619 km^2 in area, located in a deep glacial trough to the southwest of Newfoundland, Canada (DFO, 2019b). The broader channel is approximately 700 km long and 80–90 km wide and has a maximum depth of 522 m in the Cabot Strait (Todd, 2016). Within the MPA, depth ranges from 51 to 497 m with predominantly fine to mixed sediments (mud, sand, and gravel) (Lacharité et al., 2020). The area has underlying geomorphic features, including iceberg scours, pockmarks/pits, and varying slope, which have been used to classify the region into different benthoscape classes based on similarities in their features (Fig. 1; from Lacharité et al., 2020). We used a benthoscape classification layer developed by Lacharité et al. (2020), which was based on a 50-m grid resolution (bathymetry) and included mean iceberg scour density, mean pockmark/pit density and surficial sediment composition (see Table A2 for detailed descriptions of the features included in each benthoscape class, reprinted from Lacharité et al., 2020). Overall, co-located data of environmental factors and faunal presence were limited in the study area. Thus, for our study, we used the benthoscape classification layer as a potential proxy for different habitats, allowing for some semi-quantitative/qualitative analyses to identify the general spatial trends and possibly direct future sampling for quantitative analyses.

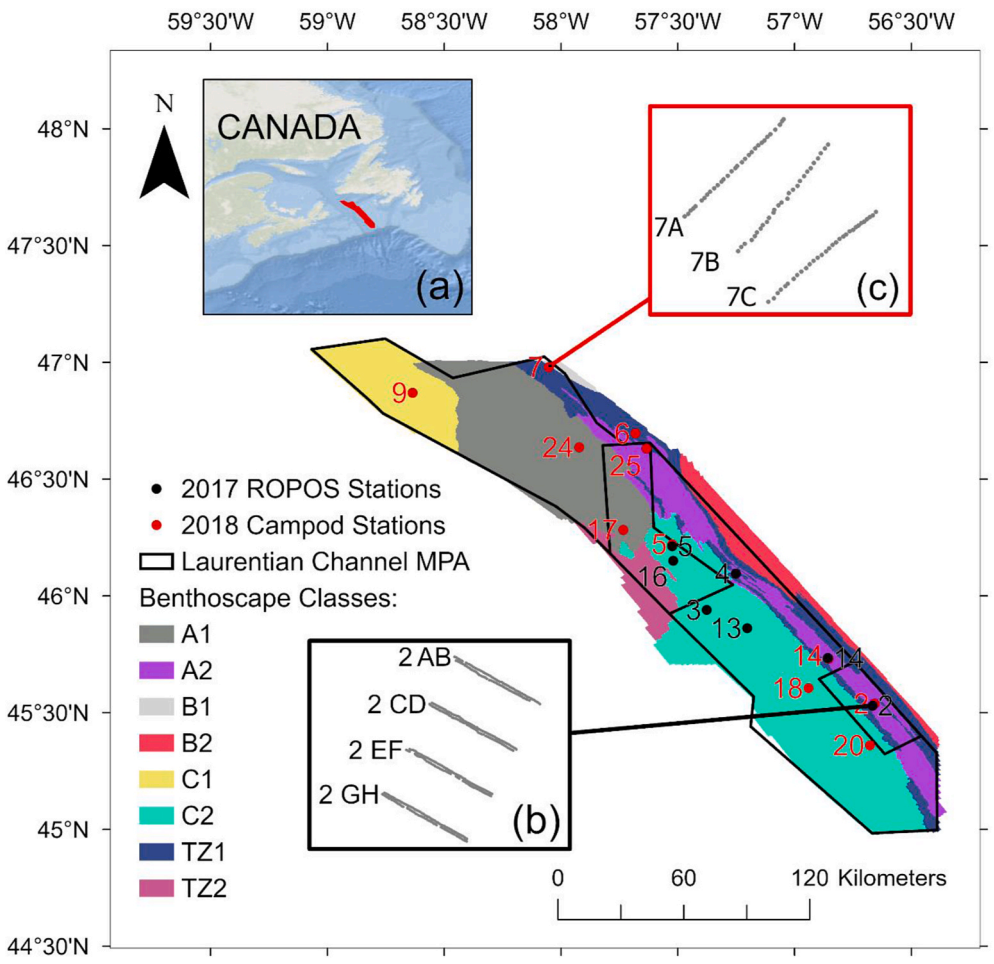

Fig. 1. Fifteen sampled stations, all, except station 6, located within the boundaries of the Laurentian Channel MPA. Co-ordinate grid in decimal degrees (WGS, 1984). Black outline indicates the outer boundary of the MPA and of the zones with specific regulations within the MPA (DFO, 2019). Black dots indicate the stations sampled by the ROV ROPOS in 2017 and red dots those sampled by the drop camera Campod in 2018. Benthoscape classes (A1-TZ2) are indicated by different colours and are based on geological variables including pockmarks, ice scours, slope, depth, and sediment; provided by Lacharité et al. (2020, Table A2). Inset (a) shows in red the MPA within the region, located southwest of Newfoundland, Canada. Inset (b) provides an example from station 2 of an array of 8 transects used to sample with ROPOS in 2017; paired 400-m transects (e.g. 2 AB, 2 CD, 2 EF, and 2 GH) were spaced 10 m apart and 200 m from the next pair. Inset (c) provides an example from station 7 of the modified transect array used to sample with Campod in 2018; 1–3 transects (e.g. 7A, 7B, and 7C) were spaced 200 m apart. Grey dots within insets (b) and (c) indicate individual image locations along each transect.

2.2. Data collection

We collected video at 7 stations (2, 3, 4, 5, 13, 14, and 16) with a downward-facing Insite Pacific Zeus-Plus HD camera (1920 × 1080 pixels) using the remotely operated vehicle ROPOS (www.ropos.com) on 9–17 September 2017. The array of sampling transects at each station included 8 400-m parallel transects spaced at alternating distances of 10 m and 200 m (i.e., four pairs of transects: AB, CD, EF, GH) (Fig. 1) for a total of 56 transects; navigation metadata was collected simultaneously (i.e., depth, altitude above seafloor, latitude, longitude). For each station, the spatial extent was ~ 0.256 km^2, including area between transects (de Mendonça and Metaxas, 2024). Our spatial design was informed using biomass data from the Department of Fisheries and Oceans Canada (DFO) multispecies trawl surveys.

In 2018, we used the drop camera Campod, a towed system with passive drifting, operated by the Department of Fisheries and Oceans Canada (DFO) [Canada, Bedford Institute of Oceanography] to collect high-resoultion still images (JPEG) at 11 stations (2, 5, 6, 7, 9, 14, 17, 18, 20, 24, and 25), with station 6 being just outside the boundary of the LC MPA on 8–11 July. Stations 2, 5, and 14 were also sampled the previous year using ROPOS. Images were captured at 10-s intervals, timed to manual hops of the camera along the seafloor, using a downward facing NIKON D810 camera (7360 × 4912 pixels). Due to limitations on time and maneuverability, we performed a modified sampling array with 1–3 transects at each station, 1-km long and spaced 200 m apart (Fig. 1) for a total of 26 transects. Navigation metadata (date, time, latitude, longitude, depth, and altitude) were provided for each image after post-processing of the Navnet, CTD, altimeter and USBL systems by the Campod technical crew. Campod had lower position accuracy of 10s of meters, compared to ~± 1 m for ROPOS. Additional specifications for both imagery tools and sampling arrays have been previously published (de Mendonça and Metaxas, 2021). The spatial extent varied with the number of transects, but was smaller than that ~ 0.256 km^2 of the ROPOS stations.

2.3. Image analysis

Overall, we aimed to avoid spatial overlap between all images included in a combined ROPOS and Campod dataset. For ROPOS, navigation metadata (using the first record per second) and video were synchronized with the Ocean Floor Observation Protocol software (OFOP 3.3.8c, Scientific Abyss Mapping Services, 2009; Huetten and Greinert, 2008). Non-overlapping images were then extracted at 1.5-m target intervals. In general, every 4th image (target interval ~ 6 m)

was selected for analysis, if near enough to the seabed (i.e., image area <6 m^2; scaling lasers spaced 10 cm apart) and image clarity permitted taxonomic identification. However, images were deemed unsuitable if they required >50% cropping to remove areas that obstructed the view of the seafloor (i.e., suspended particles, pelagic animals near the camera, sediment plumes, or sections of low light), and the next sequentially suitable image ~ 1.5–6 m was analyzed instead. This selection protocol resulted in an average of ~ 7 m spacing between analyzed images for ROPOS (grand mean ± SE: 6.94 ± 0.14 m, n = 56; range: 6.25–10.24 m). For Campod, every 4th image was a target interval of ~ 40 s and resulted in an average of ~ 14 m between analyzed images (grand mean ± SE: 14.25 ± 0.33 m, n = 26; range: 11.16–18.76 m). Although the sample size was lower for Campod than ROPOS (Table 1 and A1), the data were standardized by image area per 400-m transect to make our analyses comparable. Example imagery were provided in de Mendonça and Metaxas (2021).

Megafauna >2 cm in the largest dimension were enumerated and identified to morphotaxa, based on World Register of Marine Species (WoRMS). We calculated taxonomic numerical abundance used in all analyses, including singletons and those morphotaxa with few counts. In addition, we recorded taxa that were too numerous to count or colonial as percent cover (i.e., Elpidiidae (F.) spp., Serpulidae (F.) sp. 1, Porifera (P.) sp. 9, and Porifera (P.) sp. 23), but these were only included in the species accumulation curves that utilized presence/absence data (see Data Analyses). Highly mobile and pelagic invertebrates (e.g., malacostracans, Cephalopoda, Scyphozoa) were excluded from our study because our sampling methods were not appropriate for enumerating them, except for Elpidiidae (F.) spp., which were included only in the species accumulation curves. To describe spatial patterns, we aggregated taxa to the 10 most abundant taxonomic groups (operational cutoff of total abundance greater than 0.1 individuals/colonies m^{-2} at any station for either ROPOS or Campod), in Laurentian Channel MPA, and included an additional unique group that was very abundant at a specific station (Porifera (P.) sp. 21), with all remaining taxa aggregated into an "Other" group (40 unique taxa). We measured the spacing between image locations based on shortest linear distance (range, mean, and standard deviation/error) using ArcGIS Pro (Esri, 2020). To assess the effect of sampling on species composition, the ROPOS data were subsampled, selecting images spaced at approximately 7, 14, 21, and 28 m (grand mean ± SE: 6.94 ± 0.14, 13.97 ± 0.3, 20.97 ± 0.45, and 27.85 ± 0.58 m, n = 56).

2.4. Data Analyses

We estimated alpha and beta diversity throughout the LC MPA using count data for 63 unique taxa (e.g. Fig. 2); for species accumulation curves, we also included 4 additional taxa for which we estimated percent cover. Species accumulation curves were weighted by the area analyzed of each image for the 18 station-tool combinations, using the "random" method, 999 permutations, and confidence intervals equal to one standard deviation. We calculated Shannon diversity index by station using total abundance (individuals/colonies m^{-2}) of each taxon (Pielou, 1966).

To compare spatial patterns of the assemblages among stations and benthoscapes, we calculated Bray-Curtis dissimilarity based on total abundance of each taxon per transect (individuals/colonies m^{-2}; based on the summed counts by 63 taxa, divided by summed area per transect). One benthoscape was identified for each station, except for stations 4 and 7 where a second benthoscape was present; however, the primary benthoscape where most images were located was used for analyses. To explore the effects of benthoscape classes and stations on community structure, non-metric multi-dimensional scaling (NMDS) and permutational multivariate analysis of variance (PERMANOVA; 999 permutations) were performed using transects as sites, and 95% confidence intervals for the stations and benthoscape classes (Anderson, 2001; Kruskal, 1964). We examined how the different taxa contributed to the NMDS with the *envfit* function (999 permutations). Similarity among transects, was estimated using hierarchical clustering with the complete linkage method (Baker and Hubert, 1975) (Fig. A1). We calculated the contribution of each taxon to the average dissimilarity between stations using the Similarity Percentage method proposed in Clarke (1993), the SIMPER procedure. For very abundant taxa for which a high contribution can be an artifact of high variance, permutation tests can be used to confirm contributions (Oksanen et al., 2022). For our study, for each pairwise comparison between stations, we identified the taxa which contributed significantly (using 999 permutations and for $p < 0.05$ to unconfound abundance) by at least 10% of the cumulative percentage difference between stations.

To examine the spatial pattern (i.e. spatial range and patchiness) of

Table 1
Summary of station metadata in the Laurentian Channel MPA, including number, area, depth, altitude relative to seafloor for each image (combines 82 transects: 8 transects per ROPOS station A, B, C, D, E, F, G, and H, 1–3 transects per Campod station). Altitude refers to the height of the altimeter attached to the ROV relative to the seabed.

Station	Number of Images Analyzed	Total sum of area analyzed (m^2)	Mean Depth (m)	Standard Deviation of Depth (m)	Mean altitude above seafloor (m)	Standard deviation of altitude above seafloor (m)	Mean analyzed area per image (m^2)	Standard deviation of analyzed area per image (m^2)
ROPOS								
2	486	1033.18	350.81	2.07	1.04	0.31	2.13	0.49
3	499	739.87	445.99	0.59	0.99	0.20	1.48	0.22
4	511	862.53	335.93	2.10	1.13	0.27	1.69	0.45
5	380	592.66	439.68	0.91	1.09	0.30	1.56	0.44
13	443	574.62	432.36	1.30	1.03	0.22	1.30	0.32
14	495	616.94	343.72	1.63	1.14	0.31	1.25	0.41
16	457	464.67	444.88	1.34	1.10	0.27	1.02	0.28
Campod								
2	97	199.52	341.73	1.85	1.70	0.54	2.06	0.93
5	90*	189.78	439.89	1.15	1.60	0.38	2.11	0.65
6	59	166.76	318.72	0.59	1.62	0.29	2.83	0.92
7	90	271.02	221.18	16.35	1.67	0.34	3.01	1.02
9	55	129.66	421.84	1.75	1.53	0.24	2.36	0.69
14	63	127.39	354.40	1.23	1.76	0.42	2.02	0.76
17	29	61.16	467.47	0.82	1.61	0.32	2.11	0.84
18	93	203.83	405.26	0.96	1.58	0.35	2.19	0.70
20	58	153.78	388.21	1.16	2.33	0.86	2.65	0.77
24	96	203.32	453.47	0.85	1.45	0.28	2.12	0.66
25	60	159.82	332.67	1.20	1.57	0.28	2.66	0.86

Note: * Metadata were missing for some images, mean and standard deviation for depth and altitude calculated for N = 77 images.

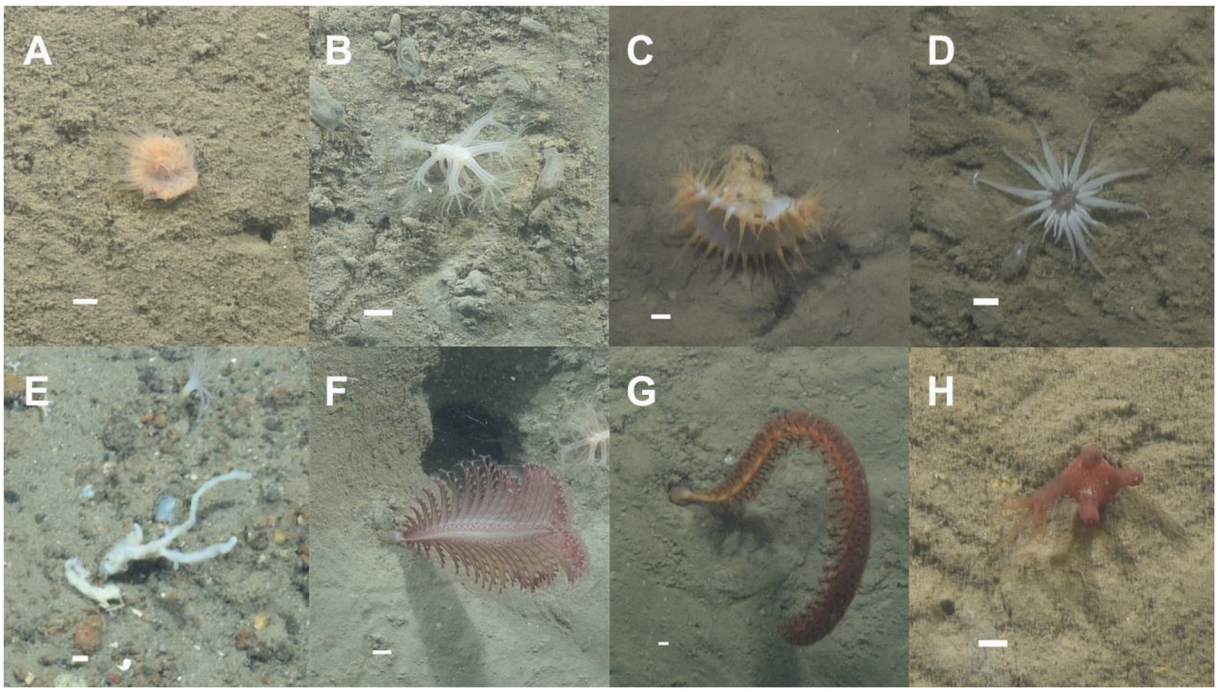

Fig. 2. Example of taxa in the Laurentian Channel MPA from Campod imagery, including A) Hexacorallia (SC.) spp. (orange to red), B) *Kophobelemnon* spp., (pink or white) C) *Actinauge cristata* (orange or white), D) *Edwardsia* sp. 1 (translucent pink or white), E) Porifera (P.) sp. 21 (amorphous; shape changes sometimes flatter), F) *Pennatula* sp. 2 (white or pink), G) *Anthoptilum* spp., and H) Anthomastinae (SF.) sp. 1. White scale bars are 1 cm, bottom left of each panel. These eight taxa are ordered from high to low contribution to pairwise station comparisons, based on the SIMPER procedure (see Table 4). Some of these taxonomic groups contain multiple morphotypes (e.g., colour varies or potentially indistinguishable species).

species assemblages, we produced Mantel correlograms, based on an ecological distance matrix with Bray-Curtis dissimilarity calculated using the abundance of each taxon (individuals/colonies m^{-2}) by image, and an Euclidean geographic distance matrix with each image location (latitude and longitude). The null hypothesis was that the distance matrices are independent (Dale and Fortin, 2014), if there are no spatial patterns in diversity. Positive Mantel values indicate positive autocorrelation of the distance matrices, where there is a similar diversity index among images at that distance class (Borcard and Legendre, 2012). Negative autocorrelation indicates the diversity index differs between images at that distance class. The spatial range of the pattern is identified at the x-intercept where the values change from positive to negative (Legendre and Fortin, 1989). Alternation of positive and negative values indicates patchiness, with a repeating pattern throughout the study area (Dale and Fortin, 2014; Legendre and Fortin, 1989).

The Mantel correlogram was computed from 999 permutations using the Spearman's *r*, with the cutoff option to limit the distance classes to include all points, and the Holm method for dealing with multiple testing problems (Holm, 1979). We included 2976 images (combined dataset for ROPOS and Campod but excluding images with zero abundance). We also computed the detrended version of the Mantel correlogram, using the residuals of Bray-Curtis after a linear model. The detrended version removes a linear trend from the species data, potentially caused by broad-scale processes or environmental gradients across the study area, to reveal finer patterns (Legendre and Fortin, 1989). We also computed a correlogram using smaller fixed distance classes of 5000 m, to help identify the spatial range of the pattern.

All statistical analyses were performed with R version 4.1.2; packages Tidyverse, Reshape, Vegan, Dendextend and Geosphere, as well as ArcGIS Pro for spacing of images (R Core Team, 2021; Esri, 2020). This study is complementary to our previous study on fine-scale spatial patterns in the Laurentian Channel MPA (de Mendonça and Metaxas, 2024).

3. Results

The highest overall abundance of taxa was at Station 2 and was ~ 4 individuals/colonies m^{-2} for ROPOS and ~ 7 individuals/colonies m^{-2} for Campod (Fig. 3). The lowest abundances were at station 5 for ROPOS (<0.5 individuals/colonies m^{-2}) and station 9 for Campod (<1 individuals/colonies m^{-2}). In addition, the composition of the community assemblage varied across the LC MPA in 4 different patterns (Fig. 3), with a large proportion of the total abundance being: for pattern (1), *Pennatula* sp. 2 and/or Hexacorallia (SC.) spp. (at station 2, 4, and 14, with Hexacorallia (SC.) spp. dominant at station 6, 20, and 25); for pattern (2) *Kophobelemnon* spp. (station 3 and 17); for pattern (3) Porifera (P.) sp. 21 (station 7); and for pattern (4) a mix of various taxa (station 5, 9, 13, 16, 18, and 24). The "Other" grouping only had a minor contribution to overall abundance, which was slightly higher at station 7 and 17 than the other stations. Overall, 11 aggregated taxonomic groups, accounting for 23 taxa, contributed to most of the megafaunal abundance in the LC MPA.

We examined spatial patterns in total abundance and taxonomic composition at 4 spatial resolutions (i.e., distances between images): 7, 14, 21, and 28 m, as well as among 8 transects with alternating spacing of 10 m and 200 m (Fig. 4). At stations where there were a few dominant taxa and high overall abundance, composition remained mostly consistent across transects and image spacings. This was the case when *Pennatula* sp. 2 and Hexacorallia (SC.) spp. were dominant and overall abundance was often ≥2 individuals/colonies m^{-2} on each transect (station 2, 4, and 14; e.g., Fig. 4A). When the number of taxonomic groups present was higher and variation across transects small, the number of transects was important for capturing diversity to avoid missing taxa. This was the case at station 3, 13, and 16, when abundance was 0.5–2 individuals/colonies m^{-2} per transect (e.g., Fig. 4B). When overall abundance was low, differences in image spacing led to different estimates of abundance, and some taxa were missed. For example, at station 5, where total abundance was often <0.5 individuals/colonies

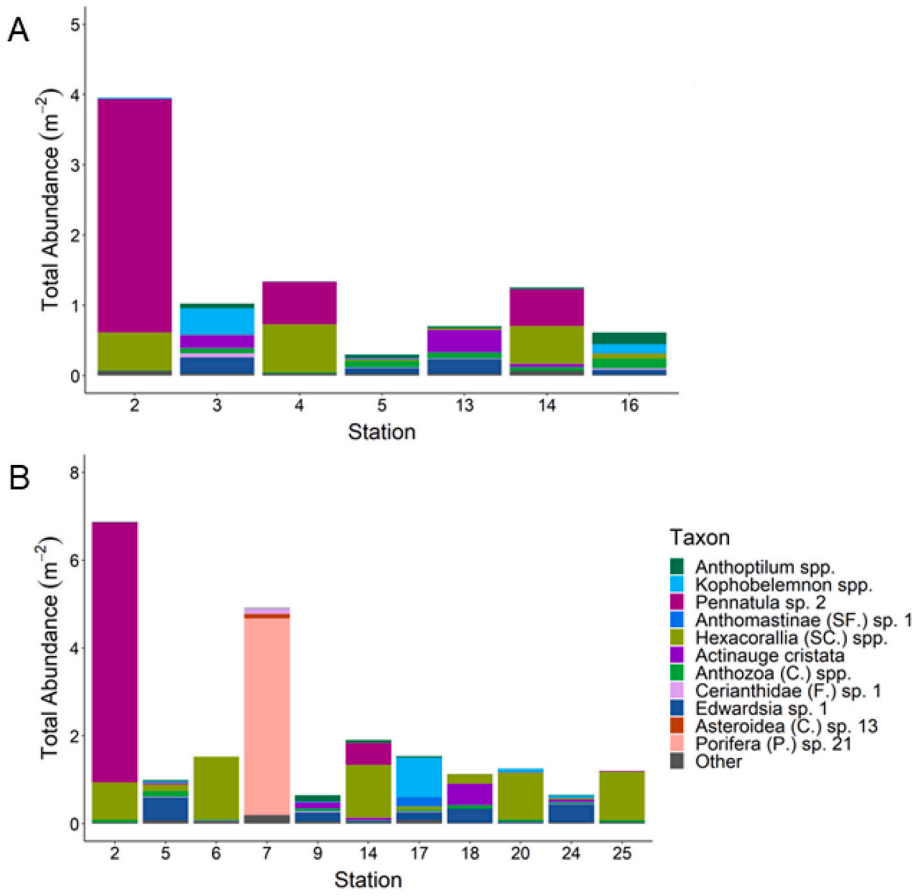

Fig. 3. Overall abundance and composition of aggregated taxa throughout the 15 Laurentian Channel MPA stations for A) ROPOS and B) Campod. Total abundance (individuals/colonies m^{-2}) calculated for each station as summed taxon counts divided by summed area analyzed. (Fig. A2 shows patterns in abundance and composition excluding the three most abundant taxa *Pennatula* sp. 2, Porifera (P.) sp. 21, and Hexacorallia (SC.) spp. that skew the scale).

m^{-2} per transect, composition varied by transect (Fig. 4C). Therefore, a higher spatial resolution with images closely spaced will likely provide more accurate estimates of abundance and capture taxa with lower abundance.

Species accumulation curves were standardized to image area (m^2), as the area and number of images varied by station (i.e., ROPOS: 380–511 images per station with area ranging 0.52–4.47 m^2 per image; Campod: 29–97 images per station with area ranging 0.75–5.40 m^2 per image). The curves using the ROPOS imagery began to approach an asymptote, with stations 2 and 3 including a higher number of morphotaxa than the other stations (Fig. 5). Most curves had a similar slope, except the one for station 3 which had the steepest slope. While no accumulation curves from the stations sampled by Campod approached an asymptote, stations 20 and 24 were nearest to reaching one. Stations 7 and 5 had the steepest slope compared to all other stations (ROPOS and Campod), capturing diversity quickly and including the highest number of species.

Shannon diversity at each station was similar for both ROPOS and Campod (Table 2). Station 5 had the highest Shannon diversity, followed by stations 16, 9, and 3. At stations where diversity was high, overall abundance (individuals/colonies m^{-2}) was often low and included relatively high abundance of *Anthoptilum* spp. and/or *Kophobelemnon* spp. (Fig. 3). The lowest Shannon diversity was found at station 6, followed by station 25 and 7. At stations where diversity was low, overall abundance was high and for a dominant taxon, e.g., Hexacorallia (SC.) spp. at stations 6 and 25, and Porifera (P.) sp. 21 at station 7 (Fig. 3).

Non-metric multi-dimensional scaling (NMDS) revealed three general groupings in the assemblages of the LC MPA (Fig. 6). These NMDS groupings were similar to the patterns identified for overall abundance (individuals/colonies m^{-2}) and composition of the numerically dominant taxa (Fig. 3). Stations 2, 4, 6, 14, 20, and 25 form a related group with the same as pattern (1) (a large proportion of *Pennatula* sp. 2 and/or Hexacorallia (SC.) spp.); and station 7 formed a separate group corresponding to pattern (3) (a large proportion of Porifera (P.) sp. 21). However, patterns (2) (a large proportion of *Kophobelemnon* spp., station 3 and 17) and (4) (a mix of various taxa at stations 5, 9, 13, 16, 18, and 24) fell under a single grouping in the NMDS. Both primary benthoscape class and station were highly significant factors affecting the groupings of the assemblages (PERMANOVA; Table 3), but primary benthoscape had a close fit to the three ordination groups (Fig. 6; 95% confidence interval ellipses). Groupings were mostly by benthoscape; benthoscapes A2 and TZ1 (stations 2, 4, 6, 14, and 25; station 20 also included yet an anomaly, as it was in benthoscape C2 but did not group with the others), benthoscape B1 (station 7), and benthoscapes A1, C1, and C2 (stations 3, 5, 9, 13, 16, 17, 18, and 24). Hierarchical clustering supported these results, but also showed that some transects clustered with different stations at lower branches, albeit still related to their station at upper branches (Fig. A1). A few taxa drove this pattern, such as Hexacorallia (SC) spp., *Kophobelemnon* spp., *Actinauge cristata*, *Edwardsia* sp. 1, Porifera (P.) sp. 21, *Pennatula* sp. 2, *Anthoptilum* spp., and Anthomastinae (SF.) sp. 1 (Table 4). Overall, 28 of the 63 taxa contributed significantly to the NMDS ($p < 0.05$), with 14 taxa being highly significant ($p = 0.001$).

For the SIMPER analyses, we focused on taxa that significantly contributed 10% or more to the ordered cumulative percentage of differences between pairs of stations. Combinations of eight taxa ranked within the top 4 at pairs, and most were also significant contributors to the NMDS, except for *Kophobelemnon* spp. and Anthomastinae (SF.) sp. 1

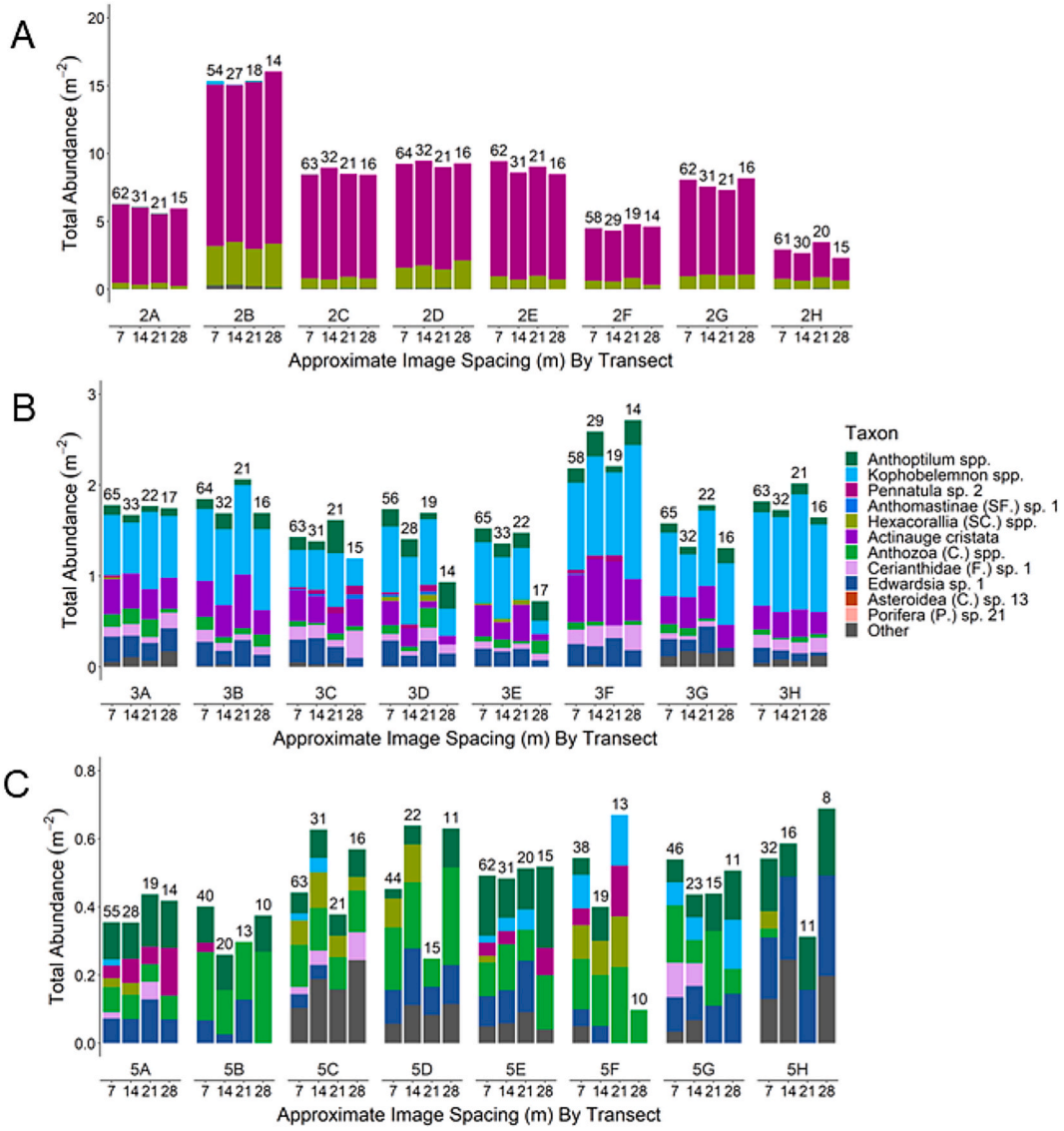

Fig. 4. Total abundance (individuals/colonies m^{-2}) of different megafaunal taxonomic groups calculated for each transect (A to H) at different spatial resolutions with spacings between images of ~ 7, 14, 21, or 28 m for A) station 2, B) station 3, and C) station 5, using ROPOS imagery. Total abundance calculated for each transect as summed taxon counts divided by summed area analyzed. Number of images are reported above each bar.

(Table 4 and Fig. 2). Most of these key taxa had relatively higher proportions compared to the rest across the LC MPA (Fig. 3; excluding Anthomastinae (SF.) sp. 1).

The first distance class in the Mantel correlogram showed positive autocorrelation (~ 4.7 km, $p = 0.001$) with communities, the study area was at that spatial distance having similar diversity indices (Bray-Curtis dissimilarity). However, the correlogram alternated between positive autocorrelation values at other distance classes (where patches had similar diversity indices), and negative autocorrelation at other distance classes (where patches had different diversity indices; Fig. 7 and Table A3). The maximum distance before the first sign change (x-intercept), which occurred around the second distance class (9.42–18.84 km), indicates the spatial range of the pattern and defines the patch size. A similar pattern was found with the detrended version of the Mantel correlogram and fixed distance classes of 5000 m, with the latter narrowing in on the spatial range of the pattern (5–10 km; Fig. A4). Overall, communities shared similarities at distances less than ~10 km (based on a Bray-Curtis dissimilarity matrix) but varied at some distances >10 km, thus, indicating patchiness in community structure throughout the LC MPA.

4. Discussion

4.1. Assemblages in the LC MPA

We detected 3 types of assemblages in the LC MPA, based on NMDS and composition [overall abundance (individuals/colonies m^{-2}) and diversity], with eight key taxa contributing to most differences. Majority of our stations (excluding 6 and 7) appeared to be within previously identified areas of high sea pen concentrations (Kenchington et al., 2010, 2016). Overall, sea pens were proportionally only dominant at a few stations. Higher abundances of *Anthoptilum* spp. and *Kophobelemnon* spp. were associated with high diversity, whereas higher abundances of *Pennatula* sp. 2 were associated with overall low diversity. These sea pens have different morphologies, but functional traits of individual species have not been assessed. Sea pens provide biogenic habitat and although known as nurseries for fish (Baillon et al., 2012), associations with epifaunal invertebrates need to be further investigated. Fish were associated with cup corals and soft corals in Alaska (Heifetz, 2002), and with cerianthids in the Gulf of Maine (Auster et al., 2003). Within the LC MPA, fish density was correlated to abundance of sea pens, cup corals,

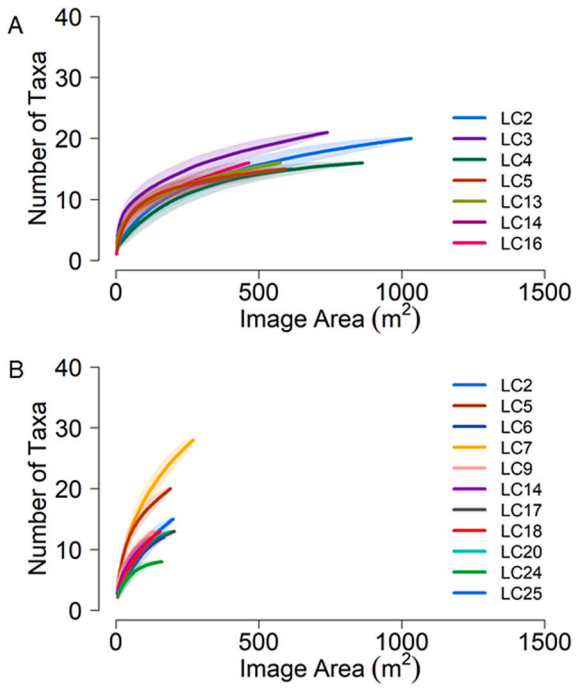

Fig. 5. Species accumulation curves by image area for each station, A) ROPOS and B) Campod, inclusive of 67 unique taxa across the Laurentian Channel MPA, using the "random" method, 999 permutations, and shaded confidence intervals of one standard deviation.

and a specific anemone/cerianthid (our Cerianthidae (F.) sp. 1) (Boulard et al., 2023).

Based on our analyses, one type of assemblage (NMDS; assemblage 1) included few dominant taxa and was detected at 6 stations (2, 4, 6, 14, 20, and 25). In all cases, overall diversity was low with *Pennatula* sp. 2 and/or Hexacorallia (SC.) spp. being dominant. While this type of assemblage had a similar range in species richness as the second type below, the Shannon diversity index differed due to variation in evenness. *Pennatula* sp. 2 may be outcompeting other epifauna in areas with suitable conditions, leading to high abundance but low diversity. In addition, *Pennatula aculeata* likely spawn continuously (Eckelbarger et al., 1998), possibly contributing to higher abundances than other species that spawn less frequently, such as *Anthoptilum grandiflorum* which spawns annually (Baillon et al., 2014). Although, Couillard et al. (2021) suggest *Pennatula aculeata* may have female biennial spawning. Hexacorallia (SC.) spp. may share a niche with *Pennatula* sp. 2, since the two taxa had an inverse trend in overall abundance. Fine-scale spatial patterns also suggest a negative association between these two corals with different local hotspots (de Mendonça and Metaxas, 2024). Abundance of *Pennatula* sp. 2 was particularly high at one station (2). Lacharité et al. (2020) also found *Pennatula* sp. in the eastern and northern parts of the Laurentian Channel (depths 265–454 m).

The second type of assemblage (NMDS; assemblage 2) included a complex mix of taxa with high overall diversity, and was detected at 8 stations (3, 5, 9, 13,16,17, 18, and 24), including the station with the highest diversity (5) in the MPA. Within this type of assemblage, patterns varied among taxa and stations. For example, *Kophobelemnon* spp. was very abundant at two stations (3 and 17), and *Anthoptilum* spp. at two different stations (9 and 16). Three additional taxa (*Actinauge cristata*, *Edwardsia* sp. 1, and Anthomastinae (SF.) sp. 1) also accounted for differences within this second type of assemblage and were more abundant in assemblage 2 than assemblage 1 (excluding Anthomastinae (SF.) sp. 1).

The third type of assemblage (NMDS; assemblage 3) occurred at a single station (7) and included several taxa that were not detected in the other assemblages. This assemblage had the second highest overall abundance and low diversity, but higher species richness than the other assemblages (low evenness). Porifera (P.) sp. 21 was the numerically dominant taxon, possibly competing with the other species. Sponges may also play an important functional role, acting as biogenic habitat (Beazley et al., 2013; Maldonado et al., 2016; McClintock et al., 2005).

Sampling designs with high spatial resolution and multiple transects are most appropriate for characterizing assemblages with high diversity. In our study, some taxa in the second assemblage were missed on specific transects and sometimes different image spacings (7, 14, 21, and 28 m) led to different estimates of abundance. Fine-scale patterns (e.g. local hotspots and variation in patch size) likely contributed to this issue (de Mendonça and Metaxas, 2024). We recommend high resolution sampling designs with multiple transects to avoid misrepresenting diversity and abundance of epifauna.

4.2. Broad-scale patterns and potential drivers

We detected some spatial structure in epifaunal diversity, reflecting a broader pattern throughout the LC MPA. Similarity in community structure (i.e. composition and diversity) appears to extend past the scale of individual stations, i.e. within ~10 km, with some differences arising at greater distances. Stations that were ~10 km apart had similar overall diversity. For example, stations 5 and 16 had similarly high diversity and stations 6 and 25 had similarly low diversity. Stations that were separated by greater distances were dissimilar (e.g. Station 6 and 16, spaced at ~ 63 km). The observed spatial structure in Bray-Curtis dissimilarity corresponded to this pattern. Ruiz-Pico et al. (2017) also detected spatial structure in sea pen aggregations in the Bay of Biscay.

Table 2
Shannon diversity ranked by station, using total abundance (individuals/colonies m^{-2}) as the summed counts of each taxon divided by summed area per station.

Rank	Station	ROPOS Dataset	Campod Dataset	Main Benthoscape	Comments and example taxon
1	5	2.01	1.81	C2	Highest Shannon Diversity; lowest overall abundance; *Anthoptilum* spp., *Edwardsia* sp. 1
2	16	1.94	–	C2	*Anthoptilum* spp., *Kophobelemnon* spp.
3	9	–	1.86	C1	*Anthoptilum* spp., *Actinauge cristata*, *Edwardsia* sp. 1
4	3	1.80	–	C2	*Anthoptilum* spp., *Kophobelemnon* spp., *Actinauge cristata*, *Edwardsia* sp. 1
5	18	–	1.80	C2	*Actinauge cristata*, *Edwardsia* sp. 1
6	13	1.51	–	C2	*Actinauge cristata*, *Edwardsia* sp. 1
7	24	–	1.45	A1	*Edwardsia* sp. 1
8	17	–	1.45	A1	*Kophobelemnon* spp.
9	14	1.35	1.17	A2	*Pennatula* sp. 2, Hexacorallia (SC.) spp.
10	4	0.95	–	A2	*Pennatula* sp. 2, Hexacorallia (SC.) spp.
11	20	–	0.95	C2	Hexacorallia (SC.) spp.
12	2	0.57	0.48	A2	*Pennatula* sp. 2, Hexacorallia (SC.) spp.; highest overall abundance
13	7	–	0.51	B1	Lots of Porifera sp. 21; shallowest station with coarser sediment
14	25	–	0.50	A2	Hexacorallia (SC.) spp.
15	6	–	0.43	TZ1	Lowest Shannon Diversity; Hexacorallia (SC.) spp.

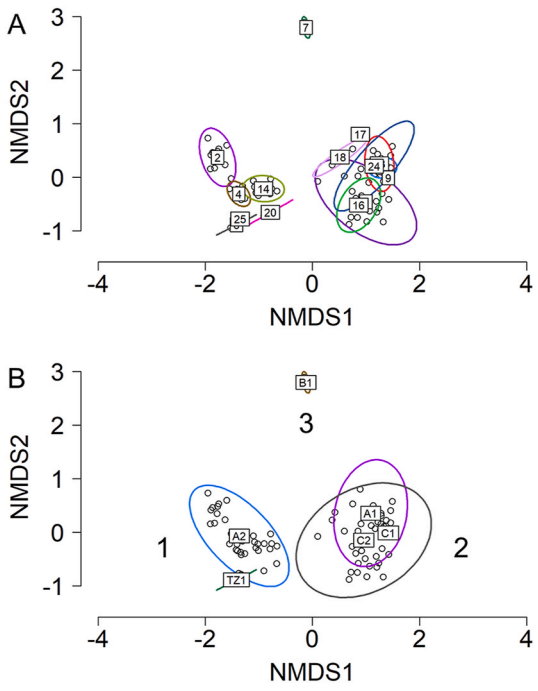

Fig. 6. Non-metric multi-dimensional scaling (NMDS) with stress of 0.109, Bray-Curtis dissimilarity using total abundance of each taxon (n = 63) per transect (individuals/colonies m^{-2}; summed counts, divided by summed area per transect). Different coloured ellipses outline the 95% confidence intervals for the groupings based on A) stations and B) primary benthoscape classes (alphanumeric labels at the center of ellipses) with labels (1–3) for the three types of assemblages. Each point represents a transect, and the number of images analyzed per transect were 32–65 for ROPOS and 25–37 for Campod. Note: At least 3 data points are needed to draw ellipses with 95% confidence intervals. For stations 6, 9, 17, 20, and 25 and benthoscape classes C1 and TZ1, there were less than 3 transects, resulting in a warning. While the ordination is valid, "ellipses" appeared as lines for groups with 2 transects or absent for station 17 with 1 transect, and thus not a true 95% confidence intervals. Also see Fig. A3 for assemblage 2.

Table 3
Permutational multivariate analysis of variance (PERMANOVA) using Bray–Curtis dissimilarity and 999 permutations, examining the effect of primary benthoscape class and station in the Laurentian Channel MPA.

Factor	df	Sums of squares	Mean Squares	*F*	R^2	*P*
Benthoscape	5	13.18	2.64	52.17	0.53	0.001*
Station	9	8.19	0.91	18.01	0.33	0.001*
Residuals	67	3.39	0.05	–	0.14	–
Total	81	24.76	–	–	1.00	–

The mantel correlogram in our study alternated between negative and positive values, suggesting a patchy pattern. Several stations harboured similar assemblage types, despite being >10 km apart, therefore supporting broad scale patchiness in community structure. Since fine-scale spatial patterns can occur (de Mendonça and Metaxas, 2024), our multiple transect design may have partially contributed to the observed patchiness. However, the study area was large enough to have environmental drivers that caused biological differences, as demonstrated by the benthoscape. Overall, broad-scale changes in community structure were apparent across the LC MPA, which was likely the result of varying spatial processes.

4.2.1. Benthoscape classes

Benthoscapes have been associated with patterns in epifaunal community structure and biodiversity (Wilson et al., 2002; Proudfoot et al., 2020). In our study, benthoscape classes were a significant factor explaining variation in community structure within the LC MPA. The classes may reflect preferred conditions or different habitats for assemblages, either directly related to geomorphology or indirectly as a proxy for covarying factors. Assemblage 1 was associated with benthoscapes A2 and TZ1, characterized as mid-depth with low relief, sparse scours, intermediate to very abundant pockmarks, and muddy/gravelly sand to mixed surficial sediment (Lacharité et al., 2020). *Pennatula* sp. 2 and/or Hexacorallia (SC.) spp. that were dominant in assemblage 1 may prefer mid-depths and low relief, possibly due to increased access to food exported from the surface waters. Assemblage 2 was associated with deep benthoscapes (C1, C2, and A1) characterized by relatively flat to low relief, sparse to very abundant scours and pockmarks, and various types of surficial sediment (fine sediment, bioturbated mud, and sandy mud with gravel traces) (Lacharité et al., 2020). The variability in geomorphic features and sediment types may be providing a wider range of habitat preferences, thus supporting the higher diversity of assemblage 2 (a complex mix of taxa). We did not sample the deep benthoscape TZ2, but Lacharité et al. (2020) suggest that it coincides with the presence of *Anthoptilum grandiflorum*, which was more prominent in deep areas of the Laurentian Channel, consistent with our results. Deep benthoscapes constitute a large portion of the MPA (combined 66% of the layer) and reflect conditions that support high epifaunal diversity (e.g. including assemblages with *Anthoptilum* spp. or *Kophobelemnon* spp). Assemblage 3 was associated with the shallow benthoscape B1, which was very steep, lacked scours, but had sparse pockmarks and coarser sediment (gravel/sandy gravel surficial sediments) (Lacharité et al., 2020). This assemblage, which was dominated by a sponge taxon, may also include additional species that prefer shallower depths and coarser sediments for attachment. Lacharité et al. (2020) described this region as one with a diverse community (e.g. sponges including *Stylocordyla* sp., crinoids, sand dollars, sea cucumbers, coralline algae, and shell debris), in contrast to our findings of overall low diversity. The specific combination of characteristics associated with different benthoscape classes appeared to correlate with differences in community structure. These individual characteristics may be correlated with spatial drivers of the observed spatial patterns in community structure.

4.2.2. Spatial drivers

Different environmental factors likely contributed as spatial drivers of the observed assemblage patterns, including depth, geological properties, physical and chemical water properties, and food, some of which were possibly captured by the benthoscape classes. We recorded lower diversity and higher overall abundance of sea pens in the eastern stations which were <400 m in depth (assemblage 1 and 3; mean depth ranges 318–388 m and 216–227 m), and higher diversity with lower abundance in western deeper stations >400 m deep (assemblage 2; mean depth ranges 405–467 m). Depth is an important driver in sea pen distributions (Ruiz-Pico et al., 2017) and modeling and observations suggest *Pennatula* is often found at shallow depths (Gullage et al., 2017; Guijarro et al., 2016; Baker et al., 2012; Langton et al., 1990). Station 2 for example, had higher mud (silt and clay) than sand (Miatta and Snelgrove, 2022), likely contributing to high abundances of *Pennatula* sp. 2 as mud is a strong predictor of the occurrence of several sea pens (Greathead et al., 2015). Lacharité et al. (2020) suggested higher abundances of sea pen towards the center of the MPA where 5 benthoscapes and thus varying sediment composition occur. In our study, relatively high abundances of *Kophobelemnon* spp. near the center of the MPA may have resulted from recruitment to preferred sediment composition (e.g. mud-sand, Baker et al., 2012) and/or other covarying factors with these benthoscapes. In other studies in the LC MPA, several environmental factors appeared to be similar in all areas where high abundances of *Pennatula* sp. 2 occurred, including the geological properties of slope, pockmarks and ice scour density, as well as point samples of bottom temperature, oxygen, salinity, and pH (de Mendonça and Metaxas, 2024; Miatta and Snelgrove, 2022). However, differences in

Table 4
Summary of SIMPER results, including the taxa that contributed at least 10% to the cumulative percentage of the difference in Bray-Curtis dissimilarity between pairs of stations. Shown are number of comparisons for which each taxon contributed to significant difference in paired station comparisons (total number pairwise comparisons: 105). Subsets of the 8 listed taxa ranked within the top 4 in all pairwise station comparisons. *envfit* p value related to the taxonomic fit of the NMDS (Fig. 6), where * is highly significant at $\alpha = 0.001$.

Taxa	Number of pairwise station comparisons for which taxon contributed to at least 10% of difference	Comments on how taxon contributed to pairwise station comparisons	*Envfit* p value (NMDS)
Hexacorallia (SC.) spp.	34	Higher abundances in assemblages in benthoscapes A2 and TZ1 (stations 4, 6, 14, or 25; excluding 2) and one in C2 (station 20) than in some combinations with the other stations except at 7.	0.001*
Kophobelemnon spp.	25	Higher abundances at stations 3 and 17 than other stations excluding 7; also, in 16 than 5 and 13, and 17 than 3 and 2.	0.007
Actinauge cristata	22	Higher abundances at stations 18 or 13 than other stations excluding 2, 7, 17; also in 3 than 5 and 16, and 9 than 5.	0.001*
Edwardsia sp. 1	21	Higher abundances at stations 18, 24, or 5 than other stations excluding 2, 3, 7, 17; also in 24 and 3 than 5, 5 than 14, and 13 than 14 and 16.	0.001*
Porifera (P.) sp. 21	14	Higher abundance at station 7 than all other stations.	0.001*
Pennatula sp. 2	12	Higher abundance at station 2 than other stations excluding 7 and 17; no other taxon had within assemblage differences for benthoscapes A2 and TZ1 (stations 2, 4, 6, 14, and 25) and one in C2 (station 20).	0.001*
Anthoptilum spp.	10	Higher abundances at stations 16 and 9 than other stations (3, 5,13,18, 20, and 24), excluding assemblages in benthoscapes A2, TZ1, and B1 (stations 2, 4, 6, 7, 14, and 25), and one in A1 (station 17).	0.001*
Anthomastinae (SF.) sp. 1	7	Higher abundance at station 17 than stations 3, 9,13,16,18, and 24 (in benthoscapes A1, C1, and C2), excluding assemblages in benthoscapes A2, TZ1, and B1 (stations 2, 4, 6, 7, 14, and 25) and one in C2 (station 20).	0.176

oxygen and/or other biochemical properties such as nutrients may arise between the northern and southern parts of the MPA over longer time scales due to ocean circulation. A warm deep (>~100–150 m, ~ 4–6 °C) water layer flows into the Laurentian channel toward the Gulf of St. Lawrence (Hebert et al., 2023; El-Sabh, 1977; Lauzier and Trites, 1958), with oxygen declining from the mouth of the Laurentian channel towards the Gulf (Gilbert et al., 2005). Chlorophyll *a* can be another strong predictor for sea pens (Gullage et al., 2017). Of the stations where *Pennatula* sp. 2 was abundant, station 2 had the second highest quantity of food (i.e. high TOM and TOC) and overall higher quality of food (i.e. high Chl *a* and TN, low C:N) (Miatta and Snelgrove, 2022).

Direct (e.g., bycatch) or indirect (e.g., sediment plumes) impacts may have reduced the past and current occurrence of vulnerable sessile species, such as sea pens. Commercial fishing activities outside the eastern and southern boundaries of the MPA and inside the MPA (Muntoni et al., 2019), may possibly impact the abundance of sea pens in nearby areas or reduce diversity. One station within assemblage 1 was located just outside the MPA boundaries (station 6) and had low diversity, suggesting that it may continue to be directly impacted by anthropogenic activities.

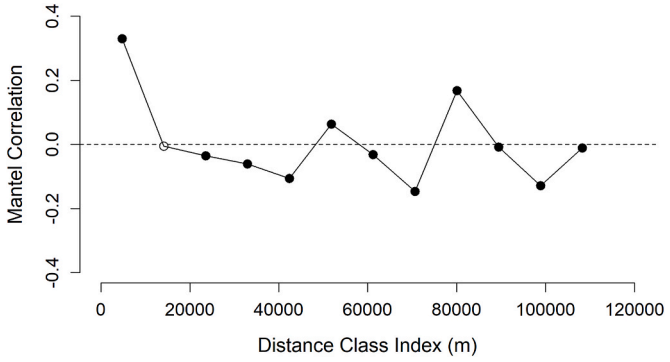

Fig. 7. Mantel correlogram based on a Brays-Curtis dissimilarity distance matrix and Euclidean distance matrix throughout the Laurentian Channel MPA, calculated from 2976 images (ROPOS and Campod combined but excluding images with zero taxon abundance). Median distance is used to represent each distance class index, which increases in increments of ~9.42 km. See appendix (Fig. A4 and Table A3) for additional details and the Mantel correlogram performed at 5000-m fixed distances. Spatial range is ~10 km. Based on 999 permutations, black points are significant and white points not significant after the Holm correction, which accounts for multiple testing.

4.3. Limitations

Sampling biases in our study could have led to differences in patterns in abundance and diversity arising as a result of unequal sample sizes (images/transects for ROPOS and Campod), tool-specific bias (de Mendonça and Metaxas, 2021), or small sampling area. Both ROVs and drop cameras are appropriate for community structure; however, an ROV can detect fine-scale patterns more accurately, as in de Mendonça and Metaxas (2024), by continuous sampling leading to higher resolution, and high maneuverability to perform standardized transect arrays. Further, species accumulation curves indicated that an area of >1000 m^2 is needed to capture the full diversity of each station. Additionally, a lack of spatial and temporal resolution in both environmental and biological data can prevent the detection and explanation of spatial trends related to the assemblages, for example by missing variation at small spatial scales within each station and having fewer distance classes between stations. Additional data at multiple spatial and temporal resolutions are needed to assess the drivers of spatial patterns in more detail, including co-located data for quantitative analysis of environmental factors.

5. Conclusion

Our study advances the knowledge of spatial patterns in the abundance (individuals/colonies m^{-2}), composition and diversity of sea pen assemblages and their potential drivers. We found that different assemblages were associated with different benthoscape classes (based on depth and geomorphic features), which in turn may provide a potentially useful proxy for different habitats. Other broad-scale drivers of epifaunal spatial patterns likely include depth or covariates, circulation, sediment properties, and food. However, additional environmental data at multiple spatial and temporal resolutions are needed to assess the importance of these drivers. Overall, adequate characterization of broad-scale patterns, including diversity and abundance, are needed to

address spatial ecology of deep-sea communities, support monitoring efforts, and allow comparisons between areas.

Funding

This research is sponsored by the NSERC Canadian Healthy Oceans Network and its Partners: Department of Fisheries and Oceans Canada and INREST (representing the Port of Sept-Îles and City of Sept-Îles); and an Natural Sciences and Engineering Research Council of Canada (NSERC) Discovery Grant (RGPIN-2021-02380) to Anna Metaxas and graduate research scholarships to Sarah N. de Mendonça (including NSERC PGS-D/CGS-D, Nova Scotia Graduate Scholarship, Faculty of Graduate Studies and President's awards Dalhousie University).

CRediT authorship contribution statement

Sarah N. de Mendonça: Writing – original draft, Visualization, Methodology, Investigation, Funding acquisition, Formal analysis, Conceptualization. **Anna Metaxas:** Writing – review & editing, Supervision, Methodology, Funding acquisition, Conceptualization.

Declaration of competing interest

The authors declare that they have no known competing financial interests or personal relationships that could have appeared to influence the work reported in this paper.

Data availability

Data are part of a thesis by SD, data will be made available on request.

Acknowledgements

We would like to acknowledge Peter Lawton (Chief Scientist) and the crews and scientists involved on the collaborative CHONe-DFO research cruises on the research vessels CCGS Hudson and CCSG Martha L. Black, with the remotely operated vehicle ROPOS and drop camera Campod, including Vonda Wareham-Hayes and Bárbara de Moura Neves (DFO-Newfoundland and Labrador for invertebrate expertise, MPA boundaries and cruise planning), Callum Mireault (deceased), Beatrice Proudfoot, Tamara Wilson, Marta Miatta, Marion Boulard, and Adam Stoer. Further, thanks to research assistants Kate Arpin (image analysis) and Jovana Kornicer (literature search/screening), as well as Craig Brown (DAL), Myriam Lacharité (UTAS), and Vicki Gazzola (DAL) for benthoscape and geomorphic feature data, and Marie-Josée Fortin (U of T) for advice on spatial statistics.

Appendix A. Supplementary data

Supplementary data to this article can be found online at https://doi.org/10.1016/j.dsr.2024.104360.

References

Anderson, M.J., 2001. A new method for non-parametric multivariate analysis of variance. Austral Ecol. 26 (1), 32–46. https://doi.org/10.1111/j.1442-9993.2001.tb00081.x.

Auster, P.J., Gjerde, K., Heupel, E., Watling, L., Grehan, A., Rogers, A.D., 2011. Definition and detection of vulnerable marine ecosystems on the high seas: problems with the "move-on" rule. ICES J. Mar. Sci. 68 (2), 254–264. https://doi.org/10.1093/icesjms/fsq074.

Auster, P.J., Lindholm, J., Valentine, P.C., 2003. Variation in habitat use by juvenile Acadian redfish, Sebastes fasciatus. Environ. Biol. Fish. 68 (4), 381–389. https://doi.org/10.1023/B:EBFI.0000005751.30906.d5.

Baillon, S., Hamel, J.F., Wareham, V.E., Mercier, A., 2012. Deep cold-water corals as nurseries for fish larvae. Front. Ecol. Environ. 10 (7), 351–356. https://doi.org/10.1890/120022.

Baillon, S., Hamel, J.F., Wareham, V.E., Mercier, A., 2014. Seasonality in reproduction of the deep-water pennatulacean coral Anthoptilum grandiflorum. Mar. Biol. 161 (1), 29–43. https://doi.org/10.1007/s00227-013-2311-8.

Baker, F.B., Hubert, L.J., 1975. Measuring the power of hierarchical cluster analysis. J. Am. Stat. Assoc. 70 (349), 31–38. https://doi.org/10.1080/01621459.1975.10480256.

Baker, K.D., Wareham, V.E., Snelgrove, P.V.R., Haedrich, R.L., Fifield, D.A., Edinger, E. N., Gilkinson, K.D., 2012. Distributional patterns of deep-sea coral assemblages in three submarine canyons off Newfoundland, Canada. Mar. Ecol. Prog. Ser. 445, 235–249. https://doi.org/10.3354/meps09448.

Beazley, L.I., Kenchington, E.L., Murillo, F.J., Sacau, M., 2013. Deep-sea sponge grounds enhance diversity and abundance of epibenthic of epibenthic megafauna in the Northwest Atlantic. ICES J. Mar. Sci. 70, 1471–1490.

Borcard, D., Legendre, P., 2012. Is the Mantel correlogram powerful enough to be useful in ecological analysis? A simulation study. Ecology 93 (6), 1473–1481. https://doi.org/10.1890/11-1737.1.

Boteler, B., Johnson, D.E., Gunn, V.K., 2023. Science for the kunming-montreal global biodiversity framework in the atlantic ocean region: an iAtlantic perspective. IAtlantic policy Br. November. https://doi.org/10.5281/zenodo.10203890.

Boulard, M., Lawton, P., Baker, K., Edinger, E., 2023. The effect of small-scale habitat features on groundfish density in deep-sea soft-bottom ecosystems. Deep. Res. Part I Oceanogr. Res. Pap. 193 (October 2022), 103891 https://doi.org/10.1016/j.dsr.2022.103891.

Chimienti, G., Angeletti, L., Rizzo, L.A.T., F, M., 2018. ROV vs trawling approaches in the study of benthic communities: the case of Pennatula rubra (Cnidaria: pennatulacea). J. Mar. Biol. Assoc. U. K. 98 (8), 1–11. https://doi.org/10.1017/S0025315418000851.

Clarke, K.R., 1993. Non-parametric multivariate analyses of changes in community structure. Aust. J. Ecol. 18 (1), 117–143. https://doi.org/10.1111/j.1442-9993.1993.tb00438.x.

Couillard, C.M., Sainte-Marie, B., Dionne, H., 2021. Late maturity and evidence for female biennial spawning in the sea pen Pennatula aculeata (Anthozoa, Pennatulacea) in eastern Canada. Invertebr. Biol. 140 (4), e12351.

Dale, M.R.T., Fortin, M.-J., 2014. Spatial Analysis : a Guide for Ecologists, second ed. Cambridge University Press. https://doi.org/10.1016/B978-0-444-53868-0.50013-7.

de Mendonça, S.N., Metaxas, A., 2021. Comparing the performance of a remotely operated vehicle, a drop camera, and a trawl in capturing deep-sea epifaunal abundance and diversity. Front. Mar. Sci. 8, 631354 https://doi.org/10.3389/fmars.2021.631354.

de Mendonça, S.N., Metaxas, A., 2024. Fine-scale spatial patterns of deep-sea epibenthic fauna in the Laurentian Channel Marine Protected area. Deep-Sea Res. Part I Oceanogr. Res. Pap. 203, 104195 https://doi.org/10.1016/j.dsr.2023.104195.

DFO, 2019. Laurentian Channel marine protected area regulations: regulatory impact analysis statement. Canada Gazette, Part 2, 153:9. http://www.gazette.gc.ca/rp-pr/p1/2017/2017-06-24/html/reg2-eng.html#footnote.595062.

Eckelbarger, K.J., Tyler, P.A., Langton, R.W., 1998. Gonadal morphology and gametogenesis in the sea pen Pennatula aculeata (Anthozoa: pennatulacea) from the Gulf of Maine. Mar. Biol. 132 (4), 677–690. https://doi.org/10.1007/s002270050432.

El-Sabh, M.I., 1977. Oceanographic features, currents, and transport in Cabot Strait. J. Fish. Res. Board Can. 34 (4), 516–528. https://doi.org/10.1139/f77-083.

Esri, 2020. ArcGIS Pro (Version 2.7.3). Esri Inc. https://www.esri.com/en-us/arcgis/products/arcgis-pro/overview (software).

Fader, G.B.J., 1991. Gas-related sedimentary features from the eastern Canadian continental shelf. Continent. Shelf Res. 11 (8–10), 1123–1153. https://doi.org/10.1016/0278-4343(91)90094-M.

Gilbert, D., Sundby, B., Gobeil, C., Mucci, A., Tremblay, G.H., 2005. A seventy-two-year record of diminishing deep-water oxygen in the St. Lawrence estuary: the northwest Atlantic connection. Limnol. Oceanogr. 50 (5), 1654–1666. https://doi.org/10.4319/lo.2005.50.5.1654.

Greathead, C., Clarke, J., Boulcott, P., Blackadder, L., Weetman, A., Wright, P.J., Gonza, J.M., 2015. Environmental requirements for three sea pen species: relevance to Distribution and Conservation. J. Mar. Sci. 72, 576–586.

Greeley, K., 2022. Skeletal Growth Ring Microanalysis and Growth Rates in (Issue January). Memorial University of Newfoundland January.

Guijarro, J., Beazley, L., Lirette, C., Kenchington, E., Wareham, V., Gilkinson, K., Alonso, M.K., Murillo, F.J., 2016. Species distribution modelling of corals and sponges from research vessel survey data in the Newfoundland and labrador region for use in the identification of significant benthic areas. J. In Can. Tech. Rep. Fish. Aquat. Sci. 3167.

Gullage, L., Devillers, R., Edinger, E., 2017. Predictive distribution modelling of cold-water corals in the Newfoundland and Labrador region. Mar. Ecol. Prog. Ser. 582, 57–77. https://doi.org/10.3354/meps12307.

Hebert, D., Layton, C., Brickman, D., Galbraith, P.S., 2023. Physical Oceanographic Conditions in the Gulf of St . Lawrence during 2022.

Heifetz, J., 2002. Coral in Alaska: distribution, abundance, and species associations. Hydrobiologia 471, 19–28. https://doi.org/10.1023/A:1016528631593.

Holm, S., 1979. A simple sequentially rejective multiple test procedure. Scand. J. Stat. 6 (2), 65–70. http://www.jstor.org/stable/4615733.

Huetten, E., Greinert, J., 2008. Software controlled guidance, recording and post-processing of seafloor observations by ROV and other towed devices: the software package OFOP. Geophys. Res. Abstr. 10. EGU2008-A-03088.

Huston, M., 1979. A general hypothesis of species diversity. Am. Nat. 113 (1), 81–101. https://doi.org/10.1086/283366.

Jones, D.O.B., Brewer, M.E., 2012. Response of megabenthic assemblages to different scales of habitat heterogeneity on the Mauritanian slope. Deep. Res. Part I Oceanogr. Res. Pap. 67, 98–110. https://doi.org/10.1016/j.dsr.2012.05.006.

Kenchington, E., Beazley, L.I., Lirette, C., Murillo, F.J., Guijarro, J., Wareham, V., Gilkinson, K., Koen-Alonso, M., Benoit, H., Bourdages, H., Sainte-Marie, B., Treble, M., Siferd, T., 2016. Delineation of coral and sponge significant benthic areas in eastern Canada using kernel density analyses and species distribution models. DFO - Can. Sci. Advis. Secr. 6 (November), 178.

Kenchington, E., Lirette, C., Cogswell, A., Archambault, D., Archambault, P., Benoit, H., Bernier, D., Brodie, B., Fuller, S., Gilkinson, K., Lévesque, M., Power, D., Siferd, T., Treble, M., Wareham, V., 2010. Delineating coral and sponge concentrations in the biogeographic regions of the east coast of Canada using spatial analyses. DFO Can. Sci. Advis. Sec. Res. Doc. 2010/041. vi + 202.

Kenchington, E., Murillo, F.J., Cogswell, A., Lirette, C., 2011. Development of encounter protocols and assessment of significant adverse impact by bottom trawling for sponge grounds and sea pen fields in the NAFO regulatory area. In: Northwest Atlantic Fisheries Organization, 11/75. NAFO SCR Doc.

Kruskal, J.B., 1964. Nonmetric multidimensional scaling: a numerical method. Psychometrika 29 (2), 115–129. https://doi.org/10.1007/BF02289694.

Lacharité, M., Brown, C.J., Normandeau, A., Todd, B.J., 2020. Geomorphic features and benthos in a deep glacial trough in Atlantic Canada. Seafloor Geomorphol. as Benthic Habitat 691–704. https://doi.org/10.1016/b978-0-12-814960-7.00041-5.

Lacharité, M., Metaxas, A., 2017. Hard substrate in the deep ocean: how sediment features influence epibenthic megafauna on the eastern Canadian margin. Deep. Res. Part I Oceanogr. Res. Pap. 126 (November 2016), 50–61. https://doi.org/10.1016/j.dsr.2017.05.013.

Langton, R.W., Langton, E.W., Theroux, R.B., Uzmann, J.R., 1990. Distribution, behavior and abundance of sea pens, Pennatula aculeata, in the Gulf of Maine. Mar. Biol. 107 (3), 463–469. https://doi.org/10.1007/BF01313430.

Lauzier, L.M., Trites, R., 1958. The deep waters in the Laurentian Channel. J. Fish. Res. Board Can. 15 (6), 1247–1257. http://www.osti.gov/servlets/purl/4290548/.

Legendre, P., Fortin, M.J., 1989. Spatial pattern and ecological analysis. Vegetatio 80 (2), 107–138. https://doi.org/10.1007/BF00048036.

Levin, L., French, S., Story, M., Jeffery, R., 2001. Environmental influences on regional deep-sea species diversity. Annu. Rev. Publ. Health 22 (1), 309–335 papers://90f132b5-cc05-44f1-a929-d329a3498f0f/Paper/p.16.

Maldonado, M., Aguilar, R., Bannister, R.J., James, J., Conway, K.W., Dayton, P.K., Cristina, D., Gutt, J., Kelly, M., Kenchington, E.L.R., Leys, S.P., Shirley, A., Tendal, O. S., Rapp, H.T., Klaus, R., Young, C.M., 2016. Sponge grounds as key marine habitats: a synthetic review of types, structure, functional roles, and conservation concerns. In: Marine Animal Forests. Springer International Publishing Switzerland, pp. 1–39. https://doi.org/10.1007/978-3-319-17001-5.

Mcclain, C.R., Schlacher, T.A., 2015. On some hypotheses of diversity of animal life at great depths on the sea floor. Mar. Ecol. 36 (4), 849–872. https://doi.org/10.1111/maec.12288.

McClintock, J.B., Amsler, C.D., Baker, B.J., Van Soest, R.W., 2005. Ecology of antarctic marine sponges : an overview. Integr. Comp. Biol. 45, 359–368.

Miatta, M., Snelgrove, P.V., 2021. Benthic nutrient fluxes in deep-sea sediments within the Laurentian Channel MPA (eastern Canada): the relative roles of macrofauna, environment, and sea pen octocorals. Deep. Res. Part I Oceanogr. Res. Pap. 178, 103655 https://doi.org/10.1016/j.dsr.2021.103655.

Miatta, M., Snelgrove, P.V.R., 2022. Sea pens as indicators of macrofaunal communities in deep-sea sediments: evidence from the Laurentian Channel marine protected area. Deep. Res. Part I Oceanogr. Res. Pap. 182 (January), 103702 https://doi.org/10.1016/j.dsr.2022.103702.

Mortensen, P.B., Buhl-Mortensen, L., Dolan, M., Dannheim, J., Kröger, K., 2009. Megafaunal diversity associated with marine landscapes of northern Norway: a preliminary assessment. Nor. Geol. Tidsskr. 89 (1–2), 163–171.

Muntoni, M., Devillers, R., Koen-Alonso, M., 2019. Science should not be left behind during the design of a marine protected area: meeting conservation priorities while integrating stakeholder interests. Facets 4, 472–492. https://doi.org/10.1139/facets-2018-0033, 2019.

Murillo, F.J., Kenchington, E., Beazley, L., Lirette, C., Knudby, A., Guijarro, J., Benoit, H., Bourdages, H., Sainte-Marie, B., 2016. Distribution modelling of sea pens, sponges, stalked tunicates and soft corals from research vessel survey data in the Gulf of St. Lawrence for use in the identification of significant benthic areas. Can. Tech. Rep. Fish. Aquat. Sci. 3170 vi + 132.

Murillo, F.J., MacDonald, B.W., Kenchington, E., Campana, S.E., Sainte-Marie, B., Sacau, M., 2018. Morphometry and growth of sea pen species from dense habitats in the Gulf of St. Lawrence, eastern Canada. Mar. Biol. Res. 1000, 1–17. https://doi.org/10.1080/17451000.2017.1417604.

Neves, B.M., Edinger, E., Layne, G.D., Wareham, V.E., 2015. Decadal longevity and slow growth rates in the deep-water sea pen Halipteris finmarchica (Sars, 1851) (Octocorallia: pennatulacea): implications for vulnerability and recovery from anthropogenic disturbance. Hydrobiologia 759 (1), 147–170. https://doi.org/10.1007/s10750-015-2229-x.

Neves, B., Edinger, E., Hayes, V.W., Devine, B., Wheeland, L., Layne, G., 2018. Size metrics, longevity, and growth rates in Umbellula encrinus (Cnidaria: pennatulacea) from the eastern Canadian Arctic. Arct. Sci. 4 (4), 722–749. https://doi.org/10.1139/as-2018-0009.

Oksanen, J., Simpson, G.L., Blanchet, F.G., Kindt, R., Legendre, P., Minchin, P.R., O'Hara, R.B., Solymos, P., Stevens, M.H.H., Szoecs, E., Wagner, H., Barbour, M., Bedward, M., Bolker, B., Borcard, D., Carvalho, G., Chirico, M., De Caceres, M., Durand, S., et al., 2022. Package "Vegan" Title Community Ecology Package. Cran, pp. 1–297.

Pielou, E.C., 1966. Shannon's formula as a measure of specific diversity: its use and misuse. Am. Nat. 100 (914), 463–465.

Proudfoot, B., Devillers, R., Brown, C.J., Edinger, E., Copeland, A., 2020. Seafloor mapping to support conservation planning in an ecologically unique fjord in Newfoundland and Labrador, Canada. J. Coast Conserv. 24, 3. https://doi.org/10.1007/s11852-020-00746-8.

Rex, M.A., 1981. Community structure in the deep-sea benthos. Annu. Rev. Ecol. Systemat. 12 (1), 331–353. https://doi.org/10.1146/annurev.es.12.110181.001555.

Ruiz-Pico, S., Serrano, A., Punzón, A., Altuna, Á., Fernández-Zapico, O., Velasco, F., 2017. Sea pen (Pennatulacea) aggregations on the northern Spanish shelf: distribution and faunal assemblages. Sci. Mar. 81 (3), 413–423. https://doi.org/10.3989/scimar.04359.06A.

Scientific Abyss Mapping Services, 2009. OFOP Documentation: Version 3.2.0k, pp. 1–42. https://www.emma-technologies.com/products/software/ofop/.

Somoza, L., Rueda, J.L., Sánchez-Guillamón, O., Medialdea, T., Rincón-Tomás, B., González, F.J., Palomino, D., Madureira, P., López-Pamo, E., Fernández-Salas, L.M., Santofimia, E., León, R., Marino, E., Fernández-Puga, M. del C., Vázquez, J.T., 2021. The interactive role of hydrocarbon seeps, hydrothermal vents and intermediate antarctic/mediterranean water masses on the distribution of some vulnerable deep-sea habitats in mid latitude NE atlantic ocean. Oceans 2 (2), 351–385. https://doi.org/10.3390/oceans2020021.

Sumida, P.Y.G., Yoshinaga, M.Y., Madureira, L.A.S.P., Hovland, M., 2004. Seabed pockmarks associated with deepwater corals off SE Brazilian continental slope. Santos Basin. Mar. Geol. 207 (1–4), 159–167. https://doi.org/10.1016/j.margeo.2004.03.006.

Swanborn, D.J.B., Huvenne, V.A.I., Malpas, T., Pittman, S.J., Rogers, A.D., Taylor, M.L., Woodall, L.C., 2023. Seamount seascape composition and configuration shape Southwest Indian Ridge fish assemblages. Deep. Res. Part I Oceanogr. Res. Pap. 191 (November 2022), 103921 https://doi.org/10.1016/j.dsr.2022.103921.

Tissot, B.N., Yoklavich, M.M., Love, M.S., York, K., Amend, M., 2006. Benthic invertebrates that form habitat on deep banks off southern California, with special reference to deep sea coral. Fish. Bull. 104 (2), 167–181.

Todd, B.J., 2016. The Laurentian Channel: a major cross-shelf trough in Atlantic Canada. Geol. Soc. Mem. 46 (1), 161–162. https://doi.org/10.1144/M46.124.

Webb, K.E., Barnes, D.K.A., Planke, S., 2009. Pockmarks: refuges for marine benthic biodiversity. Limnol. Oceanogr. 54 (5), 1776–1788. https://doi.org/10.4319/lo.2009.54.5.1776.

Wilson, M.T., Andrews, A.H., Brown, A.L., Cordes, E.E., 2002. Axial rod growth and age estimation of the sea pen, Halipteris willemoesi K??lliker. Hydrobiologia 471, 133–142. https://doi.org/10.1023/A:1016509506094.

Zajac, R.N., 2008. Challenges in marine, soft-sediment benthoscape ecology. Landsc. Ecol. 23 (Suppl. 1), 7–18. https://doi.org/10.1007/s10980-007-9140-4.